2014 International Joint Conference on Neural Networks (IJCNN)
July 6-11, 2014, Beijing, China

Decision Tree Assisted EKF for Vehicle Slip Angle Estimation Using Inertial Motion Sensors

James L. Coyte[1], Boyuan Li[1], Haiping Du[1], Weihua Li[2], David Stirling[1], Montserrat Ros[1]

***Abstract*— Vehicle side slip angle is a critical variable used in car safety systems like Electronic Stability Control. Due to the practical difficulty in direct measurement of side slip angle, accurate estimation of vehicle side slip angle using available signals is becoming important. This paper presents a novel algorithm for estimating the side slip angle of a vehicle in real time using inertial motion sensors. The algorithm uses a J48 decision tree classifier to assist the Extended Kalman Filter (EKF) predictions of the vehicle side slip angle. The decision tree classifies the inertial data into classes based on the condition the slip angle is expected to be in. Using the class information asserted by the classifier, the error covariance parameter of the EKF is adjusted to compensate for changes in disturbances and nonlinearities. The results show that the decision tree assisted EKF technique presented in this paper is capable of predicting the slip angle with sound accuracy using inertial motion data.**

I. Introduction

THE estimation of the vehicle side slip angle is an active area of research in the field of vehicle dynamics and control. The slip angle parameter is a key parameter for the safety performance of Electronic Stability Control (ESC) systems [1].

In the literature, three approaches are mainly used to estimate the side slip angle. The first method is the integration of side slip rate, which is available through the side slip rate sensor [2]. However, it is noted that the estimation performance is affected by the error from sensors biases, road grade and bank angle. The second approach that designs the observer to estimate the side slip angle needs accurate information of vehicle velocity, road friction coefficient and some tire parameters, which are hard to be directly measured [3-5]. For the third method, with the help of Global Positioning System (GPS) measurements, the side slip angle can be estimated. Ryu et al., used the combination of GPS and Inertial Navigation System (INS) to accurately estimate the side slip angle [6], but the GPS signal is not reliable due to the disturbance of satellite signals. The slip angle has been predicted in past research with the use of wheel force transducers [7], optical encoders [7], integrating Inertial Motion Sensors (IMU) with single antennae GPS [8, 9], and a single IMU [10, 11].

In general, if the vehicle state is accurately estimated, observers can be designed to estimate the side slip angle for the second method. The Kalman filter method has been extensively used to estimate the vehicle state without the requirement of tire model and road friction information. Ray conducted a series of studies on the vehicle state estimation and tire-road friction coefficient estimation [12-14]. Firstly, Ray developed a 9 degree-of-freedom (DOF) vehicle dynamics model and an analytic tire force model to simulate the real vehicle motion, and used a 5 DOF vehicle model to develop the extended Kalman filter (EKF) vehicle state estimator [12]. Then based on the developed EKF estimator in [12], the brake controller using the estimated longitudinal slip ratio was proposed [13]. Ray also suggested the extended Kalman-Bucy filtering (EKBF) and Bayesian hypothesis selection method to estimate the vehicle motion and friction coefficient [14].

Currently most practical means of measuring the side slip angle are the use of differential GPS systems which are not economical for commercial vehicles. In this paper a novel estimation algorithm is presented that has the potential to be incorporated into commercial vehicles using low cost sensors.

The problem of detecting the different conditions of slip motion can be solved using classifiers constructed using supervised learning techniques. The C4.5 algorithm is a supervised machine learning algorithm that can induce a top down decision tree that will make decisions based on patterns that occur in the data [15]. The advantage of the C4.5 algorithm is its high speed to error rate ratio [16]. An open source Java version of C4.5 is available known as the J48 algorithm [17]. In this study, Ray's EKF method is utilised along with a J48 decision tree to estimate the vehicle longitudinal velocity and lateral velocity, and the vehicle side slip angle can be estimated accordingly. The estimated side slip angle is compared with the actual value which is measured by a differential GPS and the estimation performance is verified.

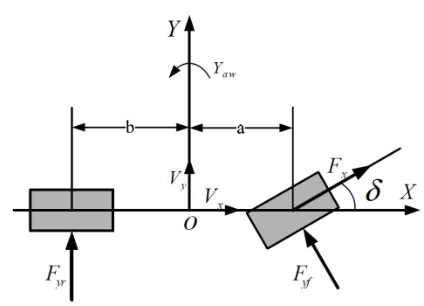

Fig.1. Simplified vehicle two wheel model.

This paper is organized as follows, Section II. gives a description of the vehicle dynamics and the EKF that is designed, Section III. provides a description on the decision

1 School of Electrical, Computer and Telecommunications Engineering Wollongong, 2500 Australia (first author's e-mail: jlc978@uowmail.edu.au).
2 School of Mechanical, Materials and Mechatronic Engineering Wollongong, 2500 Australia

tree classifier used to assist the EKF estimation, Section IV. describes the experimental procedure, Section V presents the results and discussion and the conclusion are given in section VI.

II. VEHICLE MODEL AND EKF

The objective of this project is to produce a novel estimation algorithm that can estimate the side slip angle of an automotive vehicle only using measurements from inertial motion sensors mounted to the car body and the steering wheel, that is only angular velocity and acceleration are measured. Using supervised learning, a classifier is trained with a training set of slip angle data obtained from a differential GPS. The classifier assists the EKF by making a prediction on what the process noise error is on the plant model and the noise error is on the sensors. Figure 1 illustrates a simplified model of a vehicle where δ is the wheel angle, Y_{aw} is the yaw rate. The slip angle is defined in Eq. 13 as the angle between the lateral and longitudinal velocities [18]. The simplified two wheel vehicle model is given in figure 1.

The EKF method can estimate vehicle states, like longitudinal velocity, lateral velocity and side slip angle. Based on Ray's research, the five degrees of freedom vehicle dynamics model for the EKF method, which consider the vehicle longitudinal motion, lateral motion, yaw motion and wheel dynamics, is derived as follows [2]:

$$\dot{v}_x = v_y r + \frac{1}{m}\left(F_{xf}\cos\delta_f + F_{yf}\sin\delta_f + F_{xr}\right) \tag{1a}$$

$$\dot{v}_y = -v_x r + \frac{1}{m}\left(F_{yf}\cos\delta_f - F_{xf}\sin\delta_f + F_{yr}\right) \tag{1b}$$

$$\dot{r} = \frac{1}{I_z}\left[l_f\left(F_{yf}\cos\delta_f - F_{xf}\sin\delta_f\right) - l_r F_{yr}\right] \tag{1c}$$

$$\dot{\omega}_f = \frac{1}{I_\omega}\left(-F_{xf}R_\omega + T_f\right) \tag{1d}$$

$$\dot{\omega}_r = \frac{1}{I_\omega}\left(-F_{xr}R_\omega + T_r\right) \tag{1e}$$

Where T_f and T_r are the traction torques or brake torques applied on front and rear wheel, respectively. F_{xf} and F_{xr} are front wheel and rear wheel longitudinal tire forces. F_{yf} and F_{yr} are front wheel and rear wheel lateral tire forces. δ_f is the front wheel steering angle. m denotes the vehicle mass and v_x shows the vehicle longitudinal velocity. v_y and r show the vehicle lateral velocity and yaw rate. ω_f and ω_r are the front wheel and rear wheel angular velocities. I_ω denotes the wheel moment of inertia and R_ω is the wheel radius. I_z is the vehicle moment of inertial about yaw axis. According to the vehicle dynamics model (1), the vehicle state estimator of EKF method is defined as:

$$\hat{\dot{v}}_x = \hat{v}_y r + \frac{1}{m}\left(\hat{F}_{xf}\cos\delta_f + \hat{F}_{yf}\sin\delta_f + \hat{F}_{xr}\right) \tag{2a}$$

$$\hat{\dot{v}}_y = -\hat{v}_x r + \frac{1}{m}\left(\hat{F}_{yf}\cos\delta_f - \hat{F}_{xf}\sin\delta_f + \hat{F}_{yr}\right) \tag{2b}$$

$$\hat{\dot{r}} = \frac{1}{I_z}\left[l_f\left(\hat{F}_{yf}\cos\delta_f - \hat{F}_{xf}\sin\delta_f\right) - l_r\hat{F}_{yr}\right] \tag{2c}$$

$$\hat{\dot{\omega}}_f = \frac{1}{I_\omega}\left(-\hat{F}_{xf}R_\omega + T_f\right) \tag{2d}$$

$$\hat{\dot{\omega}}_r = \frac{1}{I_\omega}\left(-\hat{F}_{xr}R_\omega + T_r\right) \tag{2e}$$

Equation (2) can be further written in the following form:

$$\dot{x} = f(x, F, u) \tag{3}$$

Where:

$$x = \begin{bmatrix} \hat{v}_x \\ \hat{v}_y \\ \hat{r} \\ \hat{\omega}_f \\ \hat{\omega}_r \end{bmatrix}, F = \begin{bmatrix} \hat{F}_{xf} & \hat{F}_{xr} & \hat{F}_{yf} & \hat{F}_{yr} \end{bmatrix} \tag{3b}$$

$$f(x,F,u) = \begin{bmatrix} \hat{v}_y r + \frac{1}{m}\left(\hat{F}_{xf}\cos\delta_f + \hat{F}_{yf}\sin\delta_f + \hat{F}_{xr}\right) \\ -\hat{v}_x r + \frac{1}{m}\left(\hat{F}_{yf}\cos\delta_f - \hat{F}_{xf}\sin\delta_f + \hat{F}_{yr}\right) \\ \frac{1}{I_z}\left[l_f\left(\hat{F}_{yf}\cos\delta_f - \hat{F}_{xf}\sin\delta_f\right) - l_r\hat{F}_{yr}\right] \\ \frac{1}{I_\omega}\left(-\hat{F}_{xf}R_\omega + T_f\right) \\ \frac{1}{I_\omega}\left(-\hat{F}_{xr}R_\omega + T_r\right) \end{bmatrix} \tag{5}$$

The discrete-time EKF is implemented by a forward Euler approximation as:

$$x(k+1) = x(k) + T \cdot f(x, u) \tag{4}$$

where T is the sampling time.
The system input is:

$$u = [\delta_f \quad T_f \quad T_r] \tag{5}$$

The measured feedback value z is defined as:

$$z = [a_x \quad a_y \quad r]^T \tag{6}$$

Where a_x and a_y are the vehicle longitudinal acceleration and lateral acceleration. The system output y is similar to z to adjust the estimation performance:

$$y = h(x, F, u) \tag{7a}$$

$$y = \begin{bmatrix} \hat{v}_y r + \frac{1}{m}\left(\hat{F}_{xf}\cos\delta_f + \hat{F}_{yf}\sin\delta_f + \hat{F}_{xr}\right) \\ -\hat{v}_x r + \frac{1}{m}\left(\hat{F}_{yf}\cos\delta_f - \hat{F}_{xf}\sin\delta_f + \hat{F}_{yr}\right) \\ \frac{1}{I_z}\left[l_f\left(\hat{F}_{yf}\cos\delta_f - \hat{F}_{xf}\sin\delta_f\right) - l_r\hat{F}_{yr}\right] \end{bmatrix} \tag{7b}$$

The system output is set same to the measured feedback value to adjust the estimation performance. After choosing the initial value for x_k^- and P_k^-, the EKF recursive algorithm can be implemented as shown in Figure 2 [19]. The left block is the time update process and the state vector can be updated by Equation (2) in discrete time. The right block is the measurement update process, which means that the state vector will be updated according to the error between the measured value and the estimated value.
A_k and H_k are the Jacobian matrices of partial derivative of $f(x, F, u)$ and $h(x, F, u)$ with respect to x.

After choosing the initial value for vehicle state x_k^- and error covariance P_k^-, the EKF recursive algorithm can be implemented [19]. First the Kalman Gain K_k can be computed in time step k:

$$K_k = P_k^- H_k^T [H_k P_k^- H_k^T + R]^{-1} \quad (8)$$

Where H_k relates the vehicle states to the measurement value and R represents the sensor error covariance matrix. Then vehicle state can be updated according to K_k:

$$x(k) = x_k^- + K_k[z(k) - h(x(k), F(k), u(k))] \quad (9)$$

And the error covariance P_k can also be updated:

$$P_k = [I - K_k H_k] P_k^- \quad (10)$$

Finally, the vehicle state and the error covariance can be updated again as the priori estimate for the next time step:

$$x_{k+1}^- = x(k) + T \cdot f\big(x(k), F(k), u(k)\big) \quad (11)$$

$$P_{k+1}^- = A_k P_k A_k^T + Q \quad (12)$$

Where Q is the process error covariance matrix.

The side slip angle β can be determined by the estimated longitudinal velocity $\hat{v}_x$ and lateral velocity $\hat{v}_y$ at the centre of gravity in the above EKF [20]:

$$\hat{\beta} = \tan^{-1}\left(\frac{\hat{v}_y}{\hat{v}_x}\right) \quad (13)$$

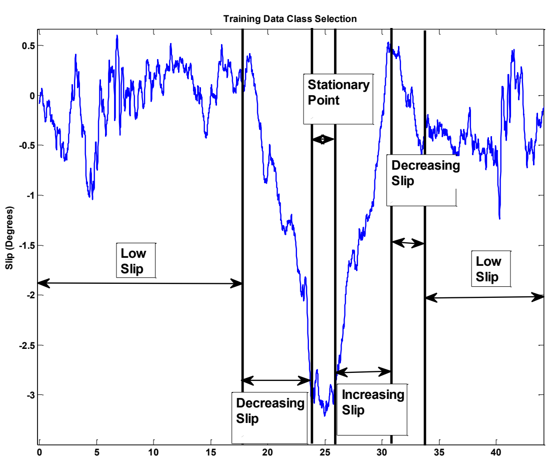

Fig. 2. GPS training data class Selection.

III. Decision Tree Classifier

The objective of the classifier is to be able to identify what category the rate of change in the slip angle the vehicle is experiencing falls into. As the dynamics of the tire is nonlinear and for this research project are not directly measured, the decision tree classifier is speculated to be an effective method for adapting to changes in disturbances and nonlinearities of the vehicle system dynamics. The four categories of slip motions are defined as 'low slip', 'decreasing slip', 'increasing slip' and 'stationary point'. Each class indicates to the EKF the value of the process noise covariance and the sensor noise covariance. Figure 3 shows the training data and assigned classes used for the j48 decision tree induction algorithm [17].

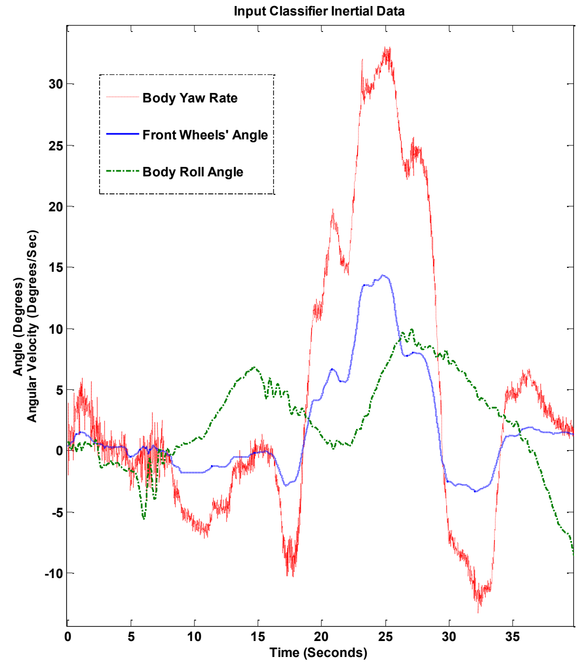

Fig. 3. Inertial training data attributes.

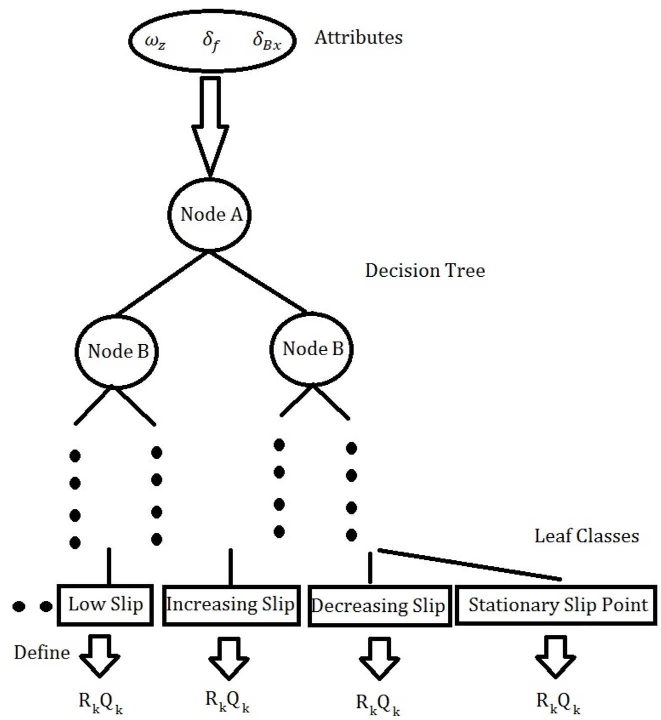

Fig. 4. Decision tree features and output classes.

Figure 3 shows the input features for the classifier that is synchronised in time with the classes shown in Figure 2. These features include the Centre of Gravity (CoG) roll angle, GoG yaw rate and the angle of the front wheels. The roll angle and yaw rate data are obtained directly from the IMU located at the GoG point of the vehicle, the front wheels' angle is calculated based on the orientation of the steering wheel. Although the roll angle measured by the IMU is not used in the vehicle model of the EKF, it is used in classifying the slip as the force on each tire is dependent on the roll angle.

Table 1
Summary of the decision tree properties

Property	J48 Tree
Training Accuracy	99.69%
Testing Accuracy	89.78%
Leaves	14
Tree Size	27

The general pseudo code for the j48 decision tree training algorithm that is used in this paper is given in Table 2. In the case of this project the attributes are the features previously mentioned, the body roll angle, yaw rate and the steering angle. The decision tree algorithm is consisted of three main steps. The first and second step is to determine the attribute with the largest normalised information gain first node of the decision tree is selected to be the node where the class with the largest normalised information gain threshold range of the base case, which is the first node of the decision tree where a relational operator that separates the data into separate groups. The final step is to recurse on the split sub sets of training data and to add these as children decision nodes.

The information gain that is calculated for each attribute in the C4.5 decision tree induction algorithm is given in eq. 16 [15]. Where equation 14 gives the measure of the average information needed to identify a class in the given training set of data T, which includes all attributes. Equation 15 is a measure of the average information of a particular attribute sub set of training data. C_j denotes the particular class corresponding to a set of training data samples in the case of this project the classes are low slip, increasing slip, and so forth. T_i denotes a particular subset of training data for a single attribute.

$$info(T) = -\sum_{j=1}^{N_{class}} \frac{freq(C_j,T)}{|T|} \times \log_2\left(\frac{freq(C_j,T)}{|T|}\right) \tag{14}$$

$$info_X(T) = \sum_{i=1}^{n} \frac{|T_i|}{|T|} \times info(T_i) \tag{15}$$

$$gain = info(T) - info_X(T) \tag{16}$$

Figure 4 shows the structure of the decision tree. Each circle represents a decision node which is a relational operator for a specific attribute where each branch represents the resultant case. Table 1 shows the performance of the decision tree.

The method used to calculate the values of the process noise and sensor noise covariance matrices is shown in figure 5. A genetic algorithm was used to calculate the R and Q values for each class of the decision tree using the GPS slip data as the reference point. The Mean Squared Error goodness of fit against the GPS training data is used as the fitness function. The trained decision tree was included within the EKF estimator.

Table 2 General pseudo code for C4.5 algorithm [16].

```
(1) Check for base cases
      For each attribute
            Calculate the information gain
            using eq. 10
(2) Let 'attribute_best' be the attribute
with the highest normalised information
gain
       Create a decision node that splits
       on 'attribute_best'
(3) Recurse on the sub-lists obtained by
splitting on 'attribute_best' and add those
nodes as children nodes
```

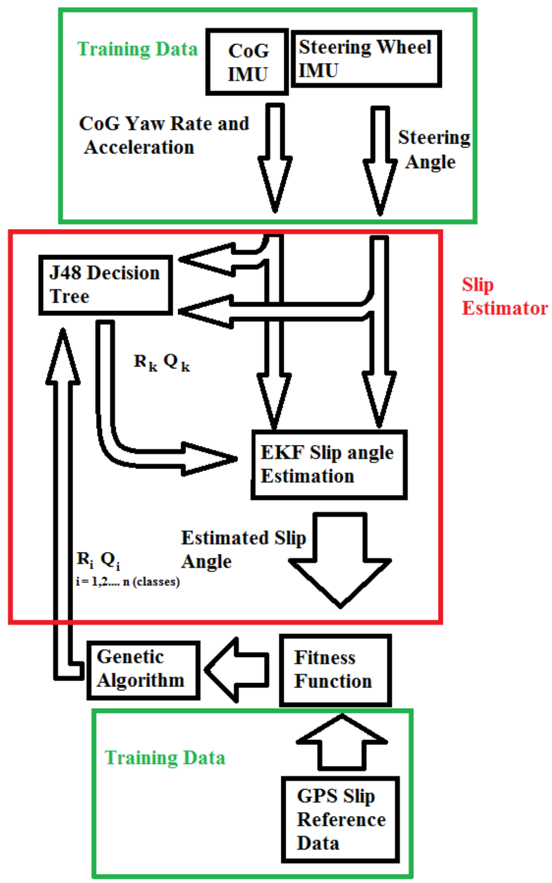

Fig. 5. Process of fine tuning the R and Q parameters

IV. Experiment

The experiment was conducted using a subcompact sedan class car, a 1986 Toyota Corolla shown in Figure 8.

The inertial motion sensors that were used for this study are 6DOF wireless MTw manufactured by Xsens [21]. Three inertial sensors are installed on the vehicle. Two are placed on the steering wheel to obtain the steering angle of the vehicle as shown in Figure 7 although only one was used whereas the second IMU served as a backup. One IMU was installed on the vehicle centre of gravity to measure the longitudinal velocity, lateral velocity, yaw rate and roll angle. The measured longitudinal acceleration, lateral acceleration, steering wheel, and yaw rate are input into the EKF estimator to estimate the vehicle side slip angle at the CoG. The key technical specifications for the IMUs are shown in Table 3.

Table 3
Technical Specifications for the MTw IMU [21].

Parameter	Value
Sampling rate	75Hz
Acceleration Dynamic Range	$\pm 160 m/s^2$
Angular velocity Dynamic Range	$\pm 1200\ °/s$
Dynamic Orientation Accuracy (RMS)	2°
Static Orientation Accuracy	1°

The roundabout test was used for this study which consisted of performing clockwise circuits around a roundabout multiple times to obtain the training data. The velocity of the vehicle is variable to suit the driving conditions, that is a value between 20 to 50 Km/h. The vehicle parameters that were used for the EKF are given in Table 4.

Table 4
Vehicle Parameters

Parameter	Description	Value
m	Vehicle mass	930 kg
I_z	Moment of inertial around z axle	1162.5 kg.m^2
l_f	Distance of C.G. from the front axle	0.972 m
l_r	Distance of C.G. from the rear axle	1.458 m
R_ω	Wheel radius	0.35 m
I_ω	Wheel moment of inertial	2.1 kg. m^2

To validate the proposed estimator, the actual slip angle is measured by a Differential GPS. The purpose of the differential GPS is to provide an accurate reference of slip angle and yaw rate data. The accuracy specifications of the GPS are presented in Table 6 [22]. The GPS antenna was mounted to the roof of the test vehicle as in Figure 7.

V. Results and Discussion

Figure 10 shows the estimated side slip angle using the testing data, which is compared with the actual value

Table 5
Performance Summary
roundabout test

	Goodness of fit		MSE	Peak Error
	NMSE	NRMSE		(°)
EKF All Data	-52.03%	-131.1%	1.5	1.12
j48-EKF Train Data	79.65%	54.89%	5.1E-05	0.0671
j48-EKF Test Data	66.26%	41.92%	6.7E-05	0.1666

measured by GPS. In this experiment, vehicle performed three successive clockwise U-turns around the same roundabout to log the training and testing data. It can be observed that for small slip angles in the regions less than 0.5 degrees, the estimated values have a larger relative error. Typical commercial ESC systems do not intervene with the steering control until the slip angle is at an unsafe level which is greater than 2° [11].

Figure 9 shows the map plot of the path the vehicle around the roundabout corresponding to the slip angle plotted in Figure 10. The maximum slip angle occurs at around 11 to 13 seconds which is in the second quadrant of the roundabout in Figure 9.

Fig. 6. Steering wheel IMU layout.

Fig. 7. Differential GPS antennae layout.

Table 6
Technical Specifications for the Vbox GPS [22]

Parameter	Value
Sampling Rate	20Hz
Velocity Accuracy	0.1 Km/h
Velocity Resolution	0.01Km/h

Fig. 8 Test vehicle 1986 Toyota Corolla.

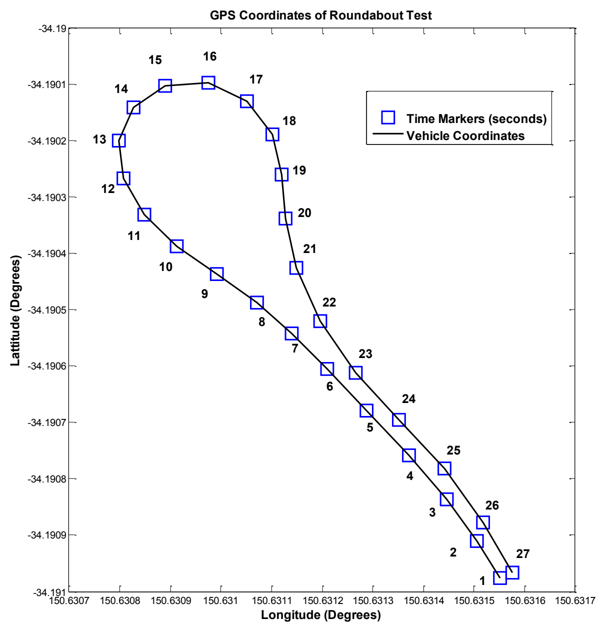

Fig. 9. Driving path map, time markers synchronised to Fig.10.

Table 5 gives a summary of the performance of the estimator. For the three turns at the round about the goodness of fit was calculated using the Normalised Mean Squared Error (NMSE) and the Normalised Root Mean Square Error (NRMS). The peak error for is the error in the maximum slip calculation at the second quadrant of the roundabout, this value was 0.166 degrees for the testing data. The training data has a much lower error due to the error covariance being directly optimised for this set of data. Figure 11 shows a comparison between the predictions produced by the standard EKF and the decision tree EKF. The standard EKF used constant noise covariance matrices and an identical vehicle model; it is shown to have a lower level of prediction accuracy. This experiment presented in this paper does not take into consideration tests on different road surface materials, driving directions or driving at higher speed, which could be a limitation of the experimental procedure presented in this paper.

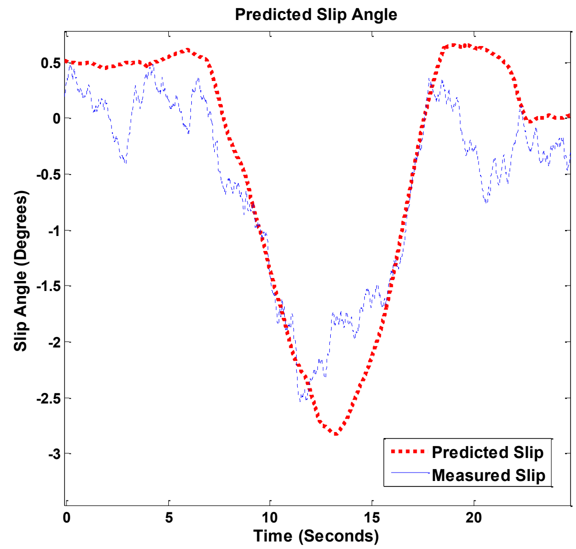

Fig. 10. Estimated and measured slip angle.

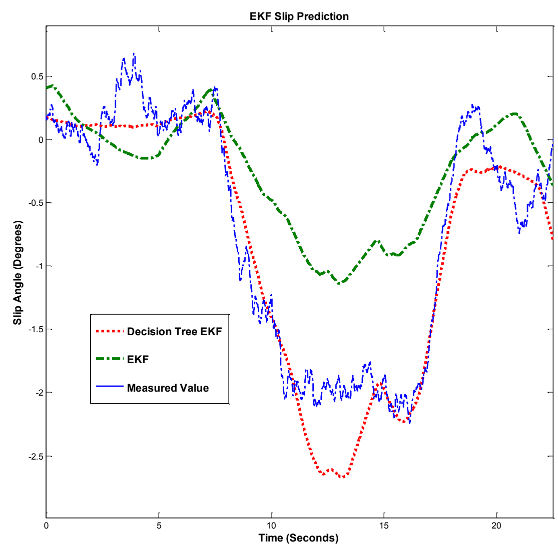

Fig. 11. Comparison between decision tree assisted EKF and EKF.

VI. Conclusions

The results of this study show that by incorporating a J48 decision tree into an EKF provides accurate estimations of the vehicle side slip angle in real time using two IMUs, without the use of GPS equipment. There is further potential to improve the classifier to identify the error covariance more accurately by making improvements to the classifier through the selection of the classes and features.

References

[1] A. T. Van Zanten, "Bosch ESP systems: 5 years of experience," *SAE transactions,* vol. 109, pp. 428-436, 2000.

[2] Y. Fukada, "Slip-Angle Estimation for Vehicle Stability Control," *Vehicle System Dynamics,* vol. 32, pp. 375-388, 1999/11/01 1999.

[3] U. Kiencke and A. Daiß, "Observation of lateral vehicle dynamics," *Control Engineering Practice,* vol. 5, pp. 1145-1150, 1997.
[4] P. J. T. Venhovens and K. Naab, "Vehicle dynamics estimation using Kalman filters," *Vehicle System Dynamics,* vol. 32, pp. 171-184, 1999.
[5] J. Stephant, A. Charara, and D. Meizel, "Virtual sensor: Application to vehicle sideslip angle and transversal forces," *Industrial Electronics, IEEE Transactions on,* vol. 51, pp. 278-289, 2004.
[6] J. Ryu, E. J. Rossetter, and J. C. Gerdes, "Vehicle sideslip and roll parameter estimation using GPS," 2002.
[7] G. Baffet, A. Charara, and D. Lechner, "Estimation of vehicle sideslip, tire force and wheel cornering stiffness," *Control Engineering Practice,* vol. 17, pp. 1255-1264, 2009.
[8] R. Daily and D. M. Bevly, "The use of GPS for vehicle stability control systems," *IEEE Transactions on Industrial Electronics,* vol. 51, pp. 270-277, 2004.
[9] J. Ryu and J. C. Gerdes, "Integrating inertial sensors with GPS for vehicle dynamics control," *Journal of Dynamic Systems, Measurement, and Control,* vol. 126, pp. 243-254, 2004.
[10] D. Piyabongkarn, R. Rajamani, J. A. Grogg, and J. Y. Lew, "Development and experimental evaluation of a slip angle estimator for vehicle stability control," *IEEE Transactions on Control Systems Technology,* vol. 17, pp. 78-88, 2009.
[11] H. Faer Grip, L. Imsland, T. A. Johansen, J. C. Kalkkuhl, and A. Suissa, "Vehicle Sideslip Estimation: DESIGN, IMPLEMENTATION, AND EXPERIMENTAL VALIDATION," *IEEE control systems,* vol. 29, pp. 36-52, 2009.
[12] L. R. Ray, "Nonlinear estimation of vehicle state and tire forces," in *American Control Conference, 1992*, 1992, pp. 526-530.
[13] L. R. Ray, "Nonlinear state and tire force estimation for advanced vehicle control," *IEEE Transactions on Control Systems Technology,* vol. 3, pp. 117-124, 1995.
[14] L. R. Ray, "Nonlinear tire force estimation and road friction identification: simulation and experiments," *Automatica,* vol. 33, pp. 1819-1833, 1997.
[15] J. R. Quinlan, *C4. 5: programs for machine learning* vol. 1: Morgan kaufmann, 1993.
[16] S. B. Kotsiantis, "Supervised machine learning: A review of classification techniques," ed, 2007.
[17] M. Hall, E. Frank, G. Holmes, B. Pfahringer, P. Reutemann, and I. H. Witten, "The WEKA data mining software: an update," *ACM SIGKDD Explorations Newsletter,* vol. 11, pp. 10-18, 2009.
[18] L. Segel, "Theoretical prediction and experimental substantiation of the response of the automobile to steering control," *Proceedings of the Institution of Mechanical Engineers: Automobile Division,* vol. 10, pp. 310-330, 1956.
[19] G. Welch and G. Bishop, "An introduction to the Kalman filter," ed, 1995.
[20] J. Dakhlallah, S. Glaser, S. Mammar, and Y. Sebsadji, "Tire-road forces estimation using extended Kalman filter and sideslip angle evaluation," in *American Control Conference, 2008*, 2008, pp. 4597-4602.
[21] G. Bellusci, F. Dijkstra, and P. Slycke, "Xsens MTw: Miniature Wireless Inertial Motion Tracker for Highly Accurate 3D Kinematic Applications," *XSENS TECHNOLOGIES,* 2013.
[22] Racelogic. (2011, 13/01/2014). "VB20SL 20Hz GPS Data Logger With Slip Angle User Guide". Available: http://www.racelogic.co.uk/_downloads/vbox/Datasheets/Data_Loggers/RLVB20SL_DATA.pdf